

## Environmental Quality Management through Parshall Flume Aeration Efficiency Modelling

Mohamed Ahmed Reda Hamed<sup>1</sup>

<sup>1</sup> Civil Engineering Department, Canadian International College, El Sheikh Zayed, Giza, Egypt  
E-mail: moha\_hamed@cic-cairo.com

### ABSTRACT

The dissolved oxygen content in surface waters is one of the vital indicators for human water quality usage as well as the aquatic plant and animal environmental life sustainability. Parshall flumes are one of the important ejector devices that are successfully used for oxygen requirement satisfying in various irrigation, wastewater, and ecosystems. However, the present study aimed to manage and improve various waterworks aeration efficiency through integrated modeling of experimental and analytical analysis as well as their operation conditional parameters for the Parshall flumes configuration. On the basis of the experiment work data sets run results, the principal component regression (PCR), partial least squares (PLS), and ridge regression (RR) techniques are used to develop the required aeration efficiency prediction models for such aerators by interrelating the impact of Parshall flumes characteristics and configurations, as well as various water flow rates on aeration efficiency. The predictive models developed in the study were statistically compared to the experimental data. The comparison confirms a good reliability and high accuracy. Considering the proposed aeration models, the optimum design of the new Parshall flumes can be successfully facilitated.

**Keywords:** aeration efficiency, dissolved oxygen, environmental life sustainability, parshall flume, and water quality.

### INTRODUCTION

Parshall flume is a modified Venturi flume with added slope to the Venturi flat bed at the throat section. It provides economical and flexible water measurement capabilities for a wide variety of open channel flow situations. (Robeson et al., 2009).

Parshall flumes are usually fabricated from three parts: The first part represents the followed by the throat part that consequently discharge the water to the third diverging part, Figure 1.

Hamed (2022) conducted experimental work to investigate the influence of venturi system properties on aeration performance. He proposed mathematical equations for prediction venturi system aeration efficiency. Al Ba'ba'a et al. (2017) conducted experimental work to determine the optimum aeration efficiency of a lab-scale air-diffused system. They investigated the influence of the orifice characteristics and configurations on the aeration efficiency.

Holler et al. (1969) developed an empirical equation for Parshall flume aeration efficiency ( $E_{20}$ ) value determination as a function of Froude number (Fr). Avery et al. (1978) carried out the experimental investigations related to Parshall flume aeration efficiency. They developed a formula for  $E_{20}$  estimation based on both Froude and Reynold numbers. Markofsky et al. (2000) investigated the effect of the Froude number on the Parshall flume aeration efficiency. Wormleaton et al. (2000) conducted an experimental work program focused on Parshall flume aeration. The results of this study revealed that  $E_{20}$  can be represented based on Froude and Reynold numbers as the main governing parameters.

Therefore, in this study, integration regression-based techniques of the principal component regression (PCR), partial least squares (PLS), and ridge regression (RR) techniques were used to develop the target Parshall flume aeration efficiency prediction models.

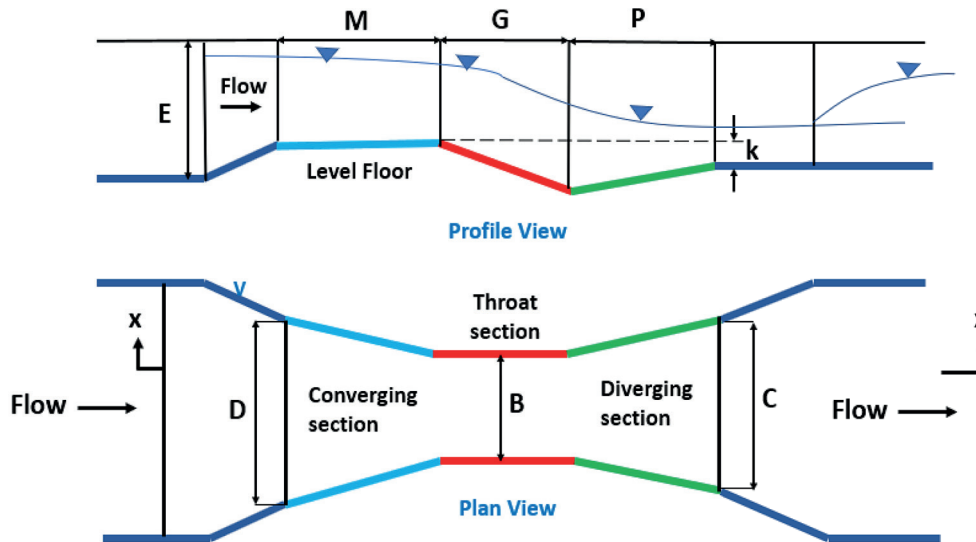


Figure 1. Parshall flume definition sketch

## AERATION MECHANISM

The oxygen transfer efficiency (aeration efficiency),  $A_E$  may be defined as:

$$A_E = (C_d - C_u)/(C_s - C_u) \quad (1)$$

where:  $u$  and  $d$  – the subscripts that indicate the upstream and downstream locations, respectively;

$C_s$  and  $C$  – the saturation concentration of oxygen in water at prevailing ambient conditions and the actual concentration of oxygen in the water.

The aeration efficiency is generally normalized to a 20 °C standard for providing a uniform basis for the comparison of measurement results. The equation that illustrates the effect of temperature is as follows (Rindels et al., 1990)

$$1 - A_{E20} = (1 - A_E)^{1/f} \quad (2)$$

where:  $A_E$  – the transfer efficiency at actual water temperature;

$A_{E20}$  – the transfer efficiency for 20 °C,  
 $T$  – the temperature;

$f$  is the exponent described as:

$$f = 1.0 + 2.1 \times 10^{-2}(T-20) + 8.26 \times 10^{-5}(T-20)^2 \quad (3)$$

## MATERIAL AND METHODS

### Experimental work

The experiments were conducted using a prismatic open rectangular channel 0.40 m wide, 0.60

m deep, and 5.00 m long. The open channels and storage tanks were made of steel plates with glass side tilting. A schematic representation of the experimental setup is shown in Figure 2. Deoxygenated water was pumped from the storage tank to stilling tank. The flow was gradually fed to the target flow rate. The discharge was measured by means of an electromagnetic flow meter installed in the supply line. At the beginning of each experiment run, the storage tank was fed with  $\text{Na}_2\text{SO}_3$  and  $\text{CoCl}_2$  for chemical de-oxygenation. During the experiments, Dissolved Oxygen (DO) measurements upstream and downstream were taken with a measuring accuracy of  $\pm 1\%$ .

Twenty-four Parshall flume models were prefabricated from steel and consequently were firmly fixed in the main experiment open rectangular channel. The dimensional details of the flume's models are presented in Table 1.

### Data sets framework

Six dominant independent variables are selected to investigate the effect of Parshall flume characteristics and configurations on its aeration efficiency ( $A_{E20}$ ) as dependent variables: Parshall discharge ( $Q$ ), throat widths ( $B$ ), throat lengths ( $G$ ), sill heights ( $K$ ), oxygen deficit ratio ( $O_g$ ), and exponent ( $f$ ), (Chau et al., 2021 and Chauhane et al., 2021). The data set consists of 96 observations were used and obtained from the laboratory experiments. Out of 96 observations, 64 arbitrarily selected observations were used for training, whereas the remaining data set (32) was used for testing the models.

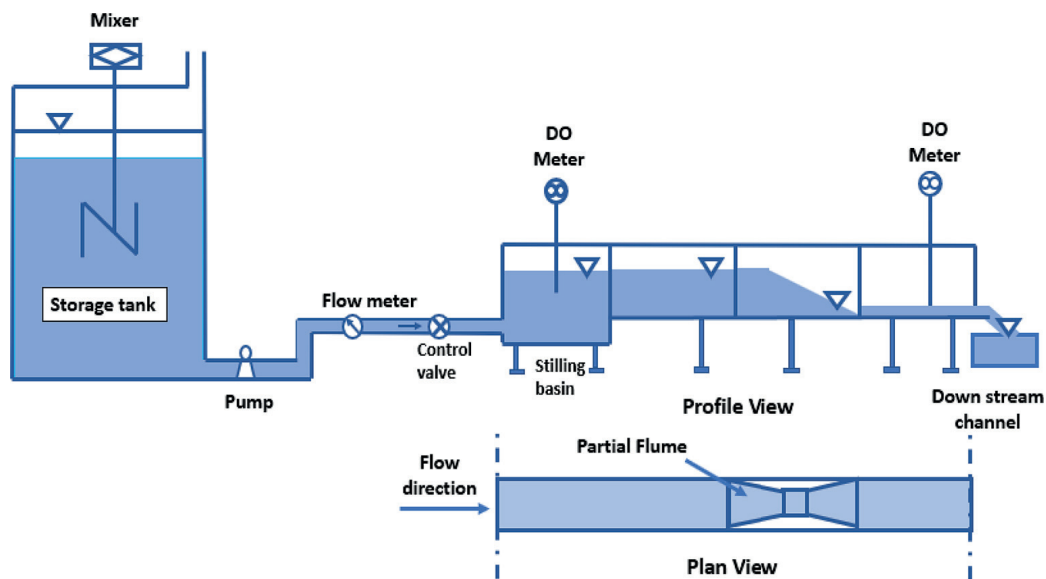


Figure 2. Experimental schematic arrangement

Table 1. Parshall flumes physical models' dimensions

Parshall flume model	B (cm)	G (cm)	K (cm)	Parshall flume model	B (cm)	G (cm)	K (cm)
PR1	2.54	7.62	1.27	PR13	5.08	12.70	1.27
PR2	2.54	7.62	2.54	PR14	5.08	12.70	2.54
PR3	2.54	7.62	3.81	PR15	5.08	12.70	3.81
PR4	2.54	7.62	5.08	PR16	5.08	12.70	5.08
PR5	2.54	10.16	1.27	PR17	7.63	12.70	1.27
PR6	2.54	10.16	2.54	PR18	7.63	12.70	2.54
PR7	2.54	10.16	3.81	PR19	7.63	12.70	3.81
PR8	2.54	10.16	5.08	PR20	7.63	12.70	5.08
PR9	5.08	10.16	1.27	PR21	7.63	15.24	1.27
PR10	5.08	10.16	2.54	PR22	7.63	15.24	2.54
PR11	5.08	10.16	3.81	PR23	7.63	15.24	3.81
PR12	5.08	10.16	5.08	PR24	7.63	15.24	5.08

### Aeration efficiency modeling techniques

In this study, three main forecasting techniques were selected to develop aeration efficiency prediction. These techniques are principal component regression (PCR), partial least squares (PLS), and ridge regression (RR).

#### Principal component regression (PCR)

PCR is one of the famous statistical techniques that are mainly used to reduce the dimension in a linear framework. However, PCR is concerned with using multiple linear regression and mathematically utilization is mainly based on the following equation, (Watson et al., 2002).

$$y_t = \beta_0 + \sum_{i=1}^p \beta_i z_{it} + \epsilon_t \quad (4)$$

where:  $y_t$  – the dependent variable (aeration efficiency),  $z_{it} \beta_i$ , and  $\epsilon_t$  – the original variable, the component weight, and estimated error respectively.

#### Partial Least Squares (PLS)

PLS is a method for relating two data matrices, X and Y, by a linear multivariate model. PLS prediction model is mainly determined based on the following equations, (Helland et al., 1990)

The first PLS component  $z_{1t}$  is defined as:

$$z_{1t} \propto \sum_{i=1}^k \text{CoV}(y_t, x_{it}) x_{it} \quad (5)$$

Next, calculate the second PLS component  $z_{2t}$  is defined as:

$$z_{2t} \propto \sum_{i=1}^k Cov(y_{1,t}, x_{1,it})x_{1,it} \quad (6)$$

The PLS linear regression is represented as:

$$y_t = \sum_{i=1}^p \beta_i z_{it} + \epsilon_t \quad (7)$$

**Ridge Regression (RR)**

The formation of ridge regression prediction model is mainly based on the following equations:

$$y_t = \hat{\beta}x_t + \epsilon_t \quad (8)$$

$$\hat{\beta}_\lambda = \underset{\beta}{\operatorname{argmin}} \left[ \sum_{t=1}^n (y_t - \hat{\beta}x_t)^2 + \lambda \hat{\beta}\hat{\beta} \right] \quad (9)$$

$$\hat{\beta}_\lambda = \left[ \sum_{t=1}^n x_t x_t' + \lambda I_k \right]^{-1} \left( \sum_{t=1}^n x_t y_t \right) \quad (10)$$

where:  $\beta$  – the coefficient vector;  
 $\lambda$  – the ridge parameter that has  $k \times k$  identity matrix and  $\lambda > 0$ .

**MODEL VALIDATION STATISTICS**

In this study, model validation statistics were implemented to evaluate its prediction accuracy. Four statistical measures are chosen to evaluate the errors in the optimum alum dose simulated results.

**Mean absolute percentage error (MAPE)**

The optimum value of MAPE for best fit simulated with regarding to the observed is zero, (Shamsi et al., 2016)]. It can be calculated according to Equation (11).

$$MAPE = \left[ \frac{1}{n} \sum_{i=1}^n |Y_{Observed} - Y_{Simulated}| / Y_{Observed} \right] \quad (11)$$

**Percent bias (PBIAS)**

The most convenient value for PBIAS is zero, (Kisi et al., 2020) [14], it can be calculated according to Equation (12):

$$PBIAS = 100 * \frac{\sum_{i=1}^n (Y_{Observed} - Y_{Simulated})}{\sum_{i=1}^n Y_{Observed}} \quad (12)$$

**Scatter index (SI)**

Scatter Index can be calculated according to Equation (13), (Yaseen et al., 2018) [15].

$$SI = \sqrt{\frac{1}{N} \sum_{i=1}^N (Y_{Observed} - Y_{Simulated})^2 / Y_{Observed}} \quad (13)$$

**Relative bias (RE)**

To evaluate the bias of simulated results from observed data, the relative t can be suitable statistical measure to evaluate the size of the bias due to under coverage with respect to the true unknown data to estimate. The relative bias can be calculated according to Equation (14).

$$RE = \left( \frac{\sum_{i=1}^N (O_i - P_i)^2}{\sum_{i=1}^N O_i} \right) \quad (14)$$

**RESULTS AND DISCUSSION**

In this experimental program, 360 runs were implemented to evaluate the influence of the Parshall flume characteristics on the aeration efficiency. After these runs, the optimum values of the experiment dominant parameters were achieved. Table 2 summaries the mean values of experimental results that were used as the main input data for the development of the predictive models.

According to the experimental aeration results, the predictive models that interrelate aeration performance as a main independent variable other Parshall flume characteristics and configurations were developed by using PCR, PLS, and RR techniques.

**Predictive models development**

*I-Principal component regressions models*

In the presence of current study’s multi collinearity data, PCR are utilized to process multiple linear regressions data. The results of a PCR are

**Table 2.** Parshall flume experimental mean results

Q	B	G	K	Og	f	A <sub>E20</sub>
60.065±24.026	5.054±1.213	10.163±3.4235	3.175±1.507	1.024±0.012	9.158±0.008	0.158±0.098

denoted in terms of principal component scores and loadings to satisfy satisfies the linear eigenvalue equation as expressed in Equation (15).

$$A_{E20} = 10^{-4} Q + 4 \cdot 10^{-4} K + 0.6978 O_g - 0.7968 \quad (15)$$

### II-Partial least squares models

Additionally, PLS was selected as important technique to develop the Parshall flume predictive model because of its reasonable accessibility to treat the missing values of data. On the basis of PLS techniques, the Aeration efficiency is driven as shown in Equation (16).

$$A_{E20} = 18.78 \cdot 10^{-5} Q + 4.33 \cdot 10^{-4} B + 7.89 \cdot 10^{-5} G + 1.36 \cdot 10^{-5} K + 61.94 \cdot 10^{-2} O_g - 1.034f + 0.2965 \quad (16)$$

### III- Ridge regression model

In this study, to permit an amount of acceptable bias tolerance in aeration efficiency prediction, ridge regression has advantage in reducing the variability of the estimated coefficients and gives a more stable and interpretable model. The ridge regression predictive model is illustrated in Equation (17).

$$A_{E20} = 10^{-4} Q + 10^{-5} G + 3.89 \cdot 10^{-4} K + 0.7657 O_g - 0.7886 \quad (17)$$

To evaluate the interrelationship between the observed and predicted values of  $A_{E20}$  at Parshall flumes, the verification plots of PCR, RR, and PLS Models is shown in Figure 3.

It can be noted a reasonable agreement between experimental aeration data and the corresponding PCR predictive model results with a correlation coefficient of 0.892. On the other hand, from the comparison of PLS and PCR models, it is obvious that a relatively improvement in correlation coefficient between observed and modelled aeration efficiency value with an approximate increasing percent of 3%. While, a relatively decreasing in the correlation coefficient value is noted by more than 4% due to applying RR techniques in comparing to PLS model.

### Models comparative evaluation and validation

To facilitate the comparative evaluation and validation of Parshall flume developed model performance, the heat-map plot is selected to clarify the relative comparison among the three denoted aeration efficiency predictive models, Figure 4. This comparison was mainly based on standardized models' parameters values.

It can be noted that the values predicted by RR model are lying significantly closer to the optimum recommended values of the four denoted evaluating statistical indicators. However, RR predictive model is the most suitable developed models for predicting  $A_{E20}$  at Parshall flumes. On the other hand, a distinctive graphical model performance evaluation was implemented based on integrated statistical measurement with the correlation coefficient as shown in Taylor diagram Figure 5.

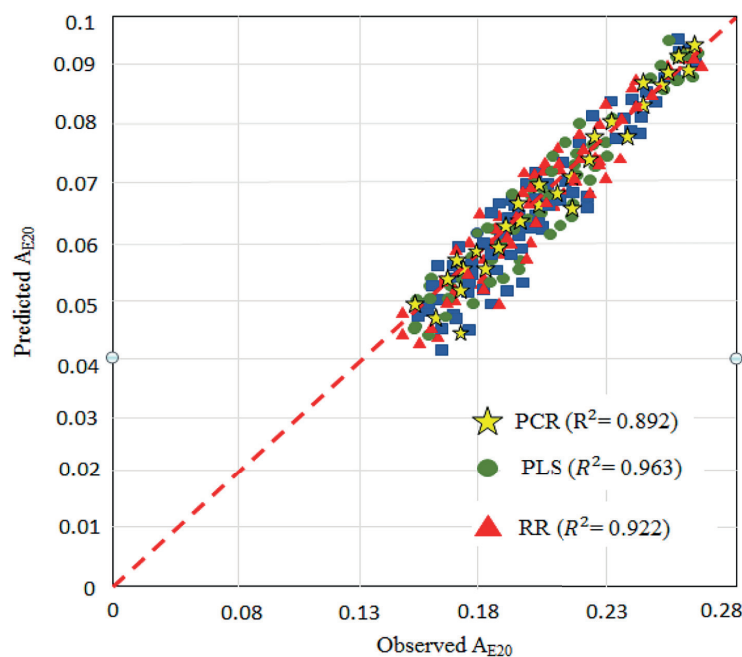


Figure 3. Observed and predicted aeration efficiency for PCR, RR, and PLS Models

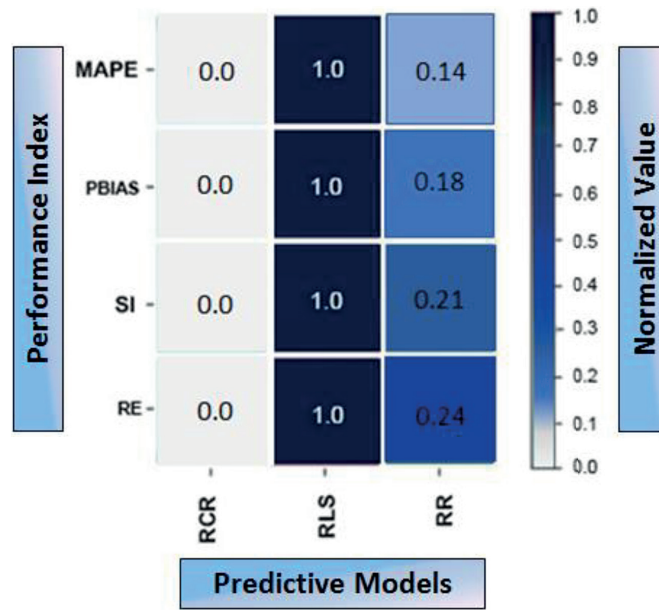


Figure 4. Predicted models heat-map plot

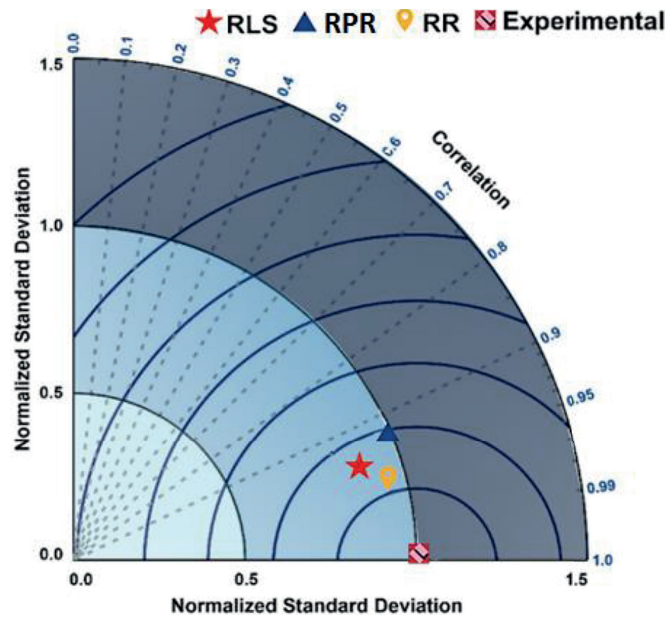


Figure 5. Taylor diagram of the predicted models

From the Taylor diagram, it is obvious confirmed that the RR model has the superior performance in aeration efficiency prediction followed by PLS model. In turn, the PCR model had the lowest accuracy in Parshall flume aeration efficiency prediction.

### CONCLUSIONS

In the experimental program of this study, 360 runs on twenty-four fabricated Parshall flume with various characteristics and configurations

were implemented to investigate their influence on the Parshall flume aeration efficiency. In this study, three main forecasting techniques were selected to develop aeration efficiency prediction. These techniques are principal component regression (PCR), partial least squares (PLS), and ridge regression (RR). The predictive models developed in the study were statistically compared to the experimental data. The comparison confirms a good reliability and high accuracy. According to the comparison of PLS and PCR models, a relative improvement in correlation coefficient between the observed and modeled

aeration efficiency value was observed with an approximate increasing percent of 3%. In turn, a relatively decreasing in the correlation coefficient value is noted by more than 4% due to applying RR techniques in comparing to PLS model. The study revealed that the RR model has the superior performance in aeration efficiency prediction, followed by PLS model. Conversely, the PCR model had the lowest accuracy in Parshall flume aeration efficiency prediction. The results indicate that the proposed predictive Parshall flume aeration efficiency models can be used for accurate water body aeration estimation, especially in the case of channels having low slopes.

## REFERENCES

1. Thornton, C.I., Smith, B.A., Abt, S.R., Robeson, M.D. 2009. Supercritical flow measurement using a small parshall flume. *Journal of Irrigation and Drainage Engineering*, 135(5), ASCE. DOI: 10.1061/(ASCE)IR.1943-4774.0000014.
2. Hamed, M.A.R. 2022. Configuration influence in relation to fluid flow of venturi system. *Environmental Quality Management, Wiley*, 1–6. DOI:10.1002/tqem.21896
3. Al Ba'ba', H. 2017. A study of optimum aeration efficiency of a lab-scale air-diffused system. *Water and Environment Journal, Wiley*, 432–439. DOI:10.1111/wej.12261
4. Preul, H.C., Holler, A.G. 2017. Reaeration through low dams in the Ohio River". In: *Proceedings of the 24<sup>th</sup> Industrial Waste Conference-Part Two*, Purdue University, Lafayette, Indiana.
5. Avery, S.T., Novak, P. 1978. Oxygen transfer at hydraulic structures. *Journal of the Hydraulics Division*, 104(11), 1521–1540. <https://doi.org/10.1061/JYCEAJ.0005100>
6. Markofsky, M., Kobus, H. 2017. Unified presentation of weir-aeration data.
7. Wormleaton, P.R., Tsang, C.C. 2000. Aeration performance of rectangular planform labyrinth weirs. *Journal of Environmental Engineering*, 126(5), 456–465. [https://doi.org/10.1061/\(ASCE\)0733-9372126:5\(456\)](https://doi.org/10.1061/(ASCE)0733-9372126:5(456))
8. Gulliver, J.S., Thene, J.R., Rindels, A.J. 1990. Indexing gas transfer in self-aerated flows. *Journal of environmental engineering*, 116(3), 503–523.
9. Sangeeta, S.B.H.S.A., Sharafati, A., Sihag, P., Al-Ansari, N., Kwok-Wing Chau K.W. 2021. Machine learning model development for predicting aeration efficiency through Parshall flume. *Engineering Applications of Computational Fluid Mechanics*, 15(1), 889–901. DOI: 10.1080/19942060.2021.1922314
10. Sihaga, P., Dursunb, O.F., Sammenc, S.S., Malikd, A., Chauhane, A. 2021. Prediction of aeration efficiency of Parshall and Modified Venturi flumes: application of soft computing versus regression models. *Engineering Applications of Computational Fluid Mechanics*, 15(1), 21(8), 2021. DOI: 10.2166/ws.2021.161 <http://creativecommons.org/licenses/by/4.0>
11. Stock, J., Watson, M. 2002. Forecasting using principal components from a large number of predictors. *Journal of the American Statistical Association*, 97, 1167–1179.
12. Helland, I. 1990. Partial least squares regression and statistical models. *Scandinavian Journal of Statistics*, 17, 97–114.
13. Parsaie, A., Najafian, S., Shamsi, Z. 2016. Predictive modeling of discharge of flow in compound open channel using radial basis neural network", *Model. Earth Syst. Environ.* <https://doi.org/10.1007/s40808-016-0207-6>.
14. Tikhamarine, Y., Malik, A., Souag-Gamane, D., Kisi, O. 2020. Artificial intelligence models versus empirical equations for modeling monthly reference evapotranspiration. *Environ", Sci. Pollut. Res.*, 27, 30001–30019. <https://doi.org/10.1007/s11356-020-08792-3>
15. Tao, H., Diop, L., Bodian, A., Djaman, K., Ndiaye, P.M., Yaseen, Z.M. 2018 Reference evapotranspiration prediction using hybridized fuzzy model with firefly algorithm: Regional case study in Burkina Faso. *Agric. Water Manag.* 208, 140–151. <https://doi.org/10.1016/j.agwat.2018.06.018>